Stretched Molecular Hydrogen Complexes of Osmium(II): A Quantum Chemical Study of the Influence of the *Trans* Ligand on Geometries, Spin–Spin Coupling Constants, Bonding, and Charge Distributions

J. S. Craw,† G. B. Bacskay,† and N. S. Hush*,†,‡

Contribution from the Department of Physical and Theoretical Chemistry and the Department of Biochemistry, University of Sydney, Sydney, N.S.W. 2006, Australia

Received December 29, 1993. Revised Manuscript Received April 1, 1994®

Abstract: A theoretical study of the stretched molecular hydrogen complexes $[Os(NH_3)_4L^z(\eta^2\text{-}H_2)]^{(z+2)+}$ ($L^z = (CH_3)_2CO$, H_2O, CH_3COO^-, Cl^-, H^-, C_5H_5N, and CH_3CN) is reported. Using SCF and MP2 methods in conjunction with effective core potentials and basis sets of triple-ζ quality on Os and double-ζ on the ligand atoms the geometries, HD spin–spin coupling constants, and binding energies have been calculated and compared with the available experimental data. The calculated H–H distances are remarkably uniform: all fall in the range 1.30–1.40 Å and correspond to stretched η^2-H_2 complexes, *i.e.* no *cis*-dihydrides have been found. The predicted H–H distance in the acetate complex is consistent with the observed distance of 1.34 Å in the ethylenediamine derivative. A unique feature of these complexes is the crucial role that electron correlation has on the H–H bond lengths; this is a consequence of the unusual potential energy surfaces that are extraordinarily flat with respect to the H–H stretch. The calculated Os–H bond lengths and stretching frequencies are also consistent with experiment. The calculated HD spin–spin coupling constants (J_{HD}) are of the same order of magnitude as those observed, yet the trend in the latter with changing *trans* ligand L^z is not adequately reproduced by the calculations, although a reasonable correlation between experimental J_{HD} and calculated H–H distance is demonstrated. In order to elucidate the nature of the Os–H_2 bonding, population analyses as well as an analysis of the binding energy of the Cl^- complex have been carried out and these further emphasize the importance of electron correlation. At the simplest level, the effect of the *trans* ligand L^z on the properties of the complexes can be related to its spectrochemical constant, which correlates with H–H distance and binding energy as well as HD spin–spin coupling constant.

I. Introduction

Since the discovery of the first η^2-H_2 complex, $W(CO)_3(P^iPr_3)_2(\eta^2\text{-}H_2)$ (^{i}Pr = isopropyl), by Kubas *et al.*[1,2] in 1984, the field of molecular hydrogen complexes has expanded rapidly. Neutron and X-ray diffraction studies[1] on this molecule have shown that the hydrogen is bound to the W in a sideways *viz.* η^2 manner. The H_2 bond length, determined from low-temperature neutron diffraction data, is 0.82 Å, *i.e.* approximately 10% longer than the equilibrium value in "free" H_2 (0.74 Å), indicating a weakening of the H_2 bond.[3,4] Kubas also found that H_2 is only weakly bound in the above complex, the enthalpy of formation being about −10 kcal/mol, and is very labile at room temperature.[5] Moreover, the η^2-H_2 complex exists in equilibrium with a seven-coordinate *cis*-dihydride. In this sense the formation of an η^2-H_2 complex can be viewed as a precursor in the oxidative addition[6] of hydrogen, although the above complex is a stable compound, *i.e.* corresponds to a minimum on the potential energy surface. Proton NMR studies have confirmed the existence of an equilibrium between such tautomers in solution,[7] and NMR has been used to probe the rotational dynamics of the bound hydrogen.[8–10] By now about

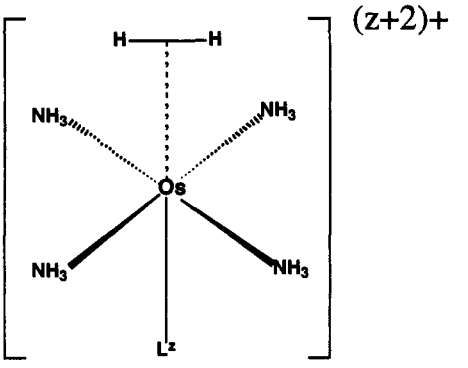

Figure 1. Structure of $[Os(NH_3)_4L^z(\eta^2\text{-}H_2)]^{(z+2)+}$.

150 molecular hydrogen complexes are known, formed from a variety of metals and ligands.

In 1971 Malin and Taube[11] reported the synthesis of the complex $[Os(en)_2H_2]^+$ (en = ethylene diamine) which is now also known to be a molecular hydrogen complex.[12] More recently, Li and Taube[12] have synthesized a series of Os(II) complexes with the general formula $[Os(NH_3)_4L^z(\eta^2\text{-}H_2)]^{(z+2)+}$ where L^z represents a range of ligands as shown in Figure 1. An interesting feature of these complexes is the considerable variation in the hydrogen–deuterium nuclear spin–spin coupling constants J_{HD} with the ligand L^z. The observed coupling constant ranges from about 20 Hz when the *trans* ligand is acetonitrile (CH_3CN) to

† Department of Physical and Theoretical Chemistry.
‡ Department of Biochemistry.
• Abstract published in *Advance ACS Abstracts,* May 15, 1994.

(1) Kubas, G. J.; Ryan, R. R.; Swanson, B. I.; Vergamini, P. J.; Wasserman, H. J. *J. Am. Chem. Soc.* **1984**, *106*, 451.
(2) Kubas, G. J. *Acc. Chem. Res.* **1988**, *21*, 120.
(3) Eckert, J.; Kubas, G. J.; Hall, J. H.; Hay, P. J.; Boyle, C. M. *J. Am. Chem. Soc.* **1990**, *112*, 2324.
(4) Kubas, G. J.; Unkefer, C. J.; Swanson, B. I.; Fukushima, E. *J. Am. Chem. Soc.* **1986**, *108*, 7000.
(5) Khalsa, G. R. K.; Kubas, G. J.; Unkefer, C. J.; Sluys, L. S. Van Der; Kubat-Martin, K. A. *J. Am. Chem. Soc.* **1990**, *112*, 3855.
(6) Crabtree, R. H.; Hlatky, G. G. *Inorg. Chem.* **1980**, *19*, 571.
(7) Desrosiers, P. J.; Cai, L.; Lin, Z.; Richards, R.; Halpern, J. *J. Am. Chem. Soc.* **1991**, *113*, 4173.
(8) Eckert, J.; Kubas, G. J.; White, R. P. *Inorg. Chem.* **1992**, *31*, 1550.
(9) Conroy-Lewis, F. M.; Simpson, S. J. *J. Chem. Soc., Chem. Commun.* **1987**, 1675.
(10) Eckert, J. *Spectrochim. Acta A* **1992**, *48*, 363.
(11) Malin, J.; Taube, H. *Inorg. Chem.* **1971**, *10*, 2403.
(12) Li, Z.-W.; Taube, H. *J. Am. Chem. Soc.* **1991**, *113*, 8946.

0002-7863/94/1516-5937$04.50/0

4 Hz when it is acetone ($(CH_3)_2CO$). This suggests a possible correlation of J_{HD} with the π donor character of the *trans* ligand (weak and strong respectively in the above example). By comparison, in "free" H_2, J_{HD} = 43 Hz.[13] Furthermore, the chemical shift for the η^2-H_2 protons appears in the spectral "window" of −20 to 0 ppm and thus is a useful diagnostic for L^z, particularly in biochemical systems.[14] The observed coupling constants are consistent with the notion that in these complexes the H_2 is considerably more stretched than in the complex $W(CO)_3(P^iPr_3)_2(\eta^2\text{-}H_2)$ where J_{HD} is 34 Hz,[1] commensurate with a marginal increase in the H_2 bond length (from 0.74 to 0.82 Å), as determined by neutron diffraction.[3]

Several other hydrogen complexes with large H–H distances (measured or inferred) have also been synthesized recently. An example is the Re polyhydride complex $ReH_7[P(C_6H_4CH_3\text{-}4)_3]_2$,[15] although it is, in fact, uncertain whether this is a true molecular hydrogen complex or a hydride in which the short H–H distances result simply from the crowding effects of bulky ligands and the high coordination number, as in the case of $[ReH_7(dppe)]$[16] (dppe = 1,2-bis(diphenylphosphino)ethane). The so called "four-legged piano-stool" complexes[17,18] are also known to exhibit H–H distances intermediate between that in free H_2 and those in classical hydrides, but chemically they behave as polyhydrides. A recent review of experimental work on molecular hydrogen complexes has been recently published by Heinekey and Oldham.[19]

A major problem in the characterization of potential η^2-H_2 complexes is discrimination between species in which an intact molecular H_2 is bound to the metal and those in which the metal has been formally oxidized to form a *cis*-dihydride. Attempts have been made to distinguish between classical (hydride) and nonclassical (η^2-H_2) structures on the basis of spin–lattice relaxation times (T_1) and it is common practice to "classify" complexes based upon whether T_1(min), the minimum in T_1 with respect to temperature, is greater than 150 ms, which is thought to indicate a classical structure, or less than 80 ms, which would correspond to a nonclassical structure, with all measurements carried out at 250 Hz. However, the overlap between the classical and nonclassical regions is considerable; thus *e.g.* some Re polyhydride complexes with classical structures exhibit fast relaxation times (<80 ms).[16,20]

Accurate experimental determination of the H–H distance in these complexes is difficult. Neutron diffraction, the most obvious technique, is hampered by the difficulty of growing good quality large crystals of dihydrogen complexes and by their high sensitivity to atmospheric oxygen. No neutron diffraction data are as yet available for the Os complexes studied in this work, although the ethylenediamine derivative of the acetate complex has been characterized.[21] Other, indirect methods that have been used to estimate the H–H distance include measurement (and interpretation) of the T_1 relaxation times and, as alluded to already, measurement of the NMR coupling constant J_{HD}. In the former it is assumed that the relaxation mechanism is of the dipole–dipole type, resulting in an inverse sixth power dependence of J_{HD} with H–H distance. An additional assumption concerns the rate of (internal) rotation of the η^2-H_2 and its relationship to the overall rate of rotation of the complex. The inferred H–H distance is strongly dependent on whether the former is assumed to be rapid or slow when compared with the overall rate of rotation.[7] For example, Desrosiers *et al.*[7] in their study of $Os(H_2)(OEP)$ (OEP = octaethylporphyrin) derive H–H distances of 1.19 and 1.49 Å depending on whether fast or slow relative rotation is assumed.

With regard to the relationship between J_{HD} and the H–H distance, an approximate empirical correlation has been proposed. In a recent review[19] a plot of J_{HD} vs H–H distance (observed or inferred) for a number of η^2-H_2 complexes clearly shows some correlation between the two quantities, although there is considerable scatter at the low J_{HD} end of the scale.

The aim of our work is the characterization of these complexes using theoretical methods, and we report the results of quantum chemical studies of the geometries, spin–spin coupling constant, and bonding. Our first calculation on the $[Os(NH_3)_4CH_3COO(\eta^2\text{-}H_2)]^+$ complex,[22] where the geometry was optimized at a level of theory that explicitly includes electron correlation (*i.e.* post self-consistent field (SCF)), led to the prediction of the very long H–H equilibrium distance of 1.39 Å, almost twice that found in H_2. This appears to be qualitatively consistent with the low value of J_{HD} = 9 Hz.[23] The SCF potential energy surface (PES) was found to be extraordinarily flat with respect to the H–H distance, and electron correlation thus plays a very important role in determining the geometry, a role which appears to be so far unique to this series of complexes. The experimental neutron diffraction value of 1.34 Å for the ethylenediamine complex,[21] which is anticipated to be closely similar to that in the tetrammine, is thus consistent with the predicted distance.

Many theoretical studies of oxidative addition can be found in the literature,[24-27] although they are mostly concerned with d^{10} Pt, Pd, and Rh complexes, where stable η^2-H_2 complexes do not seem to exist, the reactions proceeding directly to the formation of *cis*-dihydrides. In cases where η^2-H_2 structures have been found, they are usually characterized as transition states that lead to the formation of two hydride bonds with the metal, and only slightly elongated H_2 distances are predicted.[28] Maseras *et al.*[29] have performed calculations for the d^6 iron complex $[Fe(PH_3)_4H(H_2)]^+$, studying the effects of a *trans*-hydride ligand on the properties of the η^2-H_2 species; they found that H_2 was weakly bound to Fe, by only −11 kcal/mol, and that the resulting H–H distance was only marginally different from that in free H_2. Hay *et al.*[3,30,31] have carried out extensive SCF calculations on $W(CO)_3(PH_3)_2(\eta^2\text{-}H_2)$ and have reproduced most of the salient features of the $W(CO)_3(P^iPr_3)_2(\eta^2\text{-}H_2)$ complex, including the small (0.08 Å) lengthening of the H–H bond. A major feature of this species is coexistence of the η^2-H_2 and *cis*-dihydride tautomers; Hay[31] found that this equilibrium was influenced by the nature of the other ligands, *e.g.* π acceptor ligands such as CO increased the stability of the η^2-H_2 form.

The conventional theoretical model invoked to explain the bonding in molecular hydrogen complexes is essentially a one-electron picture,[30-32] analogous to that first suggested by Dewar[33] and Chatt and Duncanson[34] to interpret the bonding in metal–olefin complexes, *viz.* σ electron donation and π back-donation between ligand and metal. Thus in the Os complexes, the low-spin d^6 metal ion has an empty d_σ orbital into which the hydrogen σ bond can donate; concurrently, a doubly filled metal d_π orbital

(13) Wimmett, T. F. *Phys. Rev.* **1953**, *91*, 476.
(14) Li, Z.-W.; Taube, H. *Science* **1992**, *256*, 210.
(15) Brammer, L.; Howard, J. A. K.; Johnson, O.; Koetzle, T. F.; Spencer, J. F.; Stringer, A. M. *J. Chem. Soc., Chem. Commun.* **1991**, *4*, 241.
(16) Howard, J. A. K.; Mason, S. A.; Johnson, O.; Diamond, I. C.; Crennel, S.; Keller, P. A.; Spencer, J. L. *J. Chem. Soc., Chem. Commun.* **1988**, 1502.
(17) Poli, R. *Organometallics* **1990**, *9*, 1892.
(18) Lin, Z.; Hall, M. B. *Organometallics* **1993**, *12*, 19.
(19) Heinekey, D. M.; Oldham, W. J., Jr. *Chem. Rev.* **1993**, *93*, 913.
(20) Crabtree, R. H. *Acc. Chem. Res.* **1990**, *23*, 95.
(21) Hasegawa, T.; Koetzle, T. J.; Li, Z.; Parkin, S.; McMullan, R.; Taube, H. 29th International Conference on Coordination Chemistry, Laussane, Switzerland, 1992.
(22) Craw, J. S.; Bacskay, G. B.; Hush, N. S. *Inorg. Chem.* **1993**, *32*, 2230.
(23) Taube, H. Private communication, 1993.
(24) Low, J. J.; Goddard, W. A., III *J. Am. Chem. Soc.* **1984**, *106*, 6928.
(25) Low, J. J.; Goddard, W. A., III *J. Am. Chem. Soc.* **1984**, *106*, 8321.
(26) Obara, S.; Kitaura, K.; Morokuma, K. *J. Am. Chem. Soc.* **1984**, *106*, 7482.
(27) Koga, N.; Jin, S. Q.; Morokuma, K. *J. Am. Chem. Soc.* **1988**, *110*, 3417.
(28) Daniel, C.; Koga, N.; Han, J.; Fu, X. Y.; Morokuma, K. *J. Am. Chem. Soc.* **1988**, *110*, 3773.
(29) Maseras, F.; Duran, M.; Lledós, A.; Bertrán, J. *J. Am. Chem. Soc.* **1991**, *113*, 2879.
(30) Hay, P. J. *Chem. Phys. Lett.* **1984**, *103*, 466.
(31) Hay, P. J. *J. Am. Chem. Soc.* **1987**, *109*, 705.
(32) Saillard, J. Y.; Hoffmann, R. *J. Am. Chem. Soc.* **1984**, *106*, 2006.
(33) Dewar, M. J. S. *Bull. Soc. Chim. Fr.* **1951**, *18*, C71.
(34) Chatt, J.; Duncanson, L. A. *J. Chem. Soc.* **1953**, 2939.

can back-donate electrons into the σ^* antibonding orbital of H_2. The overall effect of such charge transfer is to lower the total energy as well as weaken (and stretch) and H_2 bond. This simple model has been used to explain the nature of bonding in the $W(CO)_3(PH_3)_2(\eta^2\text{-}H_2)$ complex quite successfully.[3]

In addition to the calculation of geometries, energies, and coupling constants, we study the bonding of molecular hydrogen in these Os complexes with a view to assessing the importance of the above charge transfer mechanism, both at the SCF and correlated levels of theory.

II. Theoretical and Computational Methods

Effective core potential (ECP) techniques are used in the quantum chemical calculations that are parametrized so that relativistic corrections are accounted for. The basis sets and effective core potentials chosen are those of Stoll *et al.*[35,36] The Os set consists of a contracted [5s4p3d] Gaussian basis set to accommodate the valence *ns*,*np*,*nd* ($n = 5$) electrons. This ECP is preferred to other commonly used potentials, for example,[37,38] as the *ns* and *np* electrons are explicitly included in the valence shell (*i.e.* are not part of the ECP). Hay *et al.*[3] have remarked on the necessity of including the 5s and 5p electrons explicitly in order to predict the correct metal–hydrogen bond length. Moreover, the valence basis sets of Stoll *et al.*[35,36] are considerably more flexible than those of Hay and Wadt[38] or Stevens *et al.*[39] For the carbon, nitrogen, oxygen, and chlorine atoms non-relativistic ECP's are used and the basis sets are [2s2p] contracted Gaussians. A double-ζ basis set[40] is used for the hydrogens, with one set of 2p functions ($\zeta_p = 0.8$) added to the molecular H_2 and the hydride ligand in the $[Os(NH_3)_4H(\eta^2\text{-}H_2)]^+$ complex in order to improve the description of their interaction with Os. It should be noted that SCF test calculations we have made show that use of the "compact" basis sets of Stevens *et al.*[39] lead to results similar to those obtained with the basis of Stoll *et al.*[35,36]

The quantum chemical calculations reported in this work have been performed mostly at the Hartree–Fock SCF and second-order Møller–Plesset perturbation (MP2) levels of theory. It was not possible, unfortunately, to optimize the geometries at the MP2 level using analytic gradients; nevertheless, a method was devised so that the H–H and Os–H distances would be determined at the correlated (MP2) level. Such a procedure is justified by the fact that only the H–H distance is particularly sensitive to inclusion of correlation. Our approach has been to optimize the geometry with respect to all internal coordinates at the SCF level for fixed values of the H–H and Os–H distances, followed by a single-point MP2 calculation at the resulting geometry. Thus a discrete two-dimensional representation of the potential energy surface is obtained with respect to these two parameters, from which their equilibrium values are readily determined. This technique was used previously for the acetate complex.[22]

The nuclear spin–spin coupling constant J_{AB} describing the magnetic interaction between nuclei A and B can be formulated as a derivative of the energy,[41,42] *viz.*

$$J_{AB} = \frac{h\gamma_A\gamma_B}{4\pi^2}\left.\frac{\partial^2 E(\mu_A,\mu_B)}{\partial\mu_A\partial\mu_B}\right|_{\mu_A=0,\mu_B=0} \tag{1}$$

where γ_A and γ_B are the magnetogyric ratios of nuclei A and B with magnetic moments μ_A and μ_B. As shown by Pople *et al.*,[41,42] and more recently by Kowalewski *et al.*[43–45] as well as Sekino and Bartlett,[46] the derivative itself can be readily calculated using the finite perturbation method within the framework of the unrestricted Hartree–Fock (UHF) formalism. This technique is used in our work also, calculating, as suggested by Kowalewski *et al.*,[45] the derivative via the simple difference formula

$$\left.\frac{\partial^2 E(\lambda_A,\lambda_B)}{\partial\lambda_A\partial\lambda_B}\right|_{\lambda_A=0,\lambda_B=0} \approx [E(\lambda_A,\lambda_B) - E(\lambda_A,-\lambda_B)]/2\lambda_A\lambda_B \tag{2}$$

where λ_A and λ_B are finite, suitably large, "effective" magnetic moments and $E(\lambda_A,\lambda_B)$ is the total molecular energy calculated in the presence of the finite perturbation H_{AB} that expresses the spin–spin interaction. It is generally recognized that the dominant mechanism of interaction for H–H coupling is the Fermi contact term;[47,48] thus, in line with other studies, we calculate only the Fermi contact contribution to the coupling constant. Thus the perturbing Hamiltonian is

$$H_{AB} = \lambda_A H_A^{fc} + \lambda_B H_B^{fc} \tag{3}$$

where

$$H_A^{fc} = \frac{16}{3}\pi\beta\sum_{k=1}^{n}\delta(r_k - r_A)I_z(A)\cdot S_z(k) \tag{4}$$

represents the contact interaction between nucleus A and the electrons. In eq 4, $I_z(A)$ is the z component of the nuclear spin angular momentum of nucleus A, r_A represents its coordinates, $S_z(k)$ is the z component of the spin angular momentum of the kth electron, with coordinates r_k, and β is the Bohr magneton.

Other methods that could be used to calculate coupling constants within the framework of the SCF formulation include the coupled perturbed Hartree–Fock (CPHF) method and techniques such as single excitation configuration interaction (SX-CI) and random phase approximation (RPA), where the manifold of triplet excited states are explicitly calculated. We have implemented the CPHF approach,[49–51] whereby we solve the inhomogeneous linear equations

$$^3\mathbf{H}\mathbf{C}(A) = -\mathbf{V}(A) \tag{5}$$

where $\mathbf{V}(A)$ represents the perturbation by the magnetic moment of nucleus A, its elements defined as

$$V(A)_{ai} = \frac{16}{3}\pi\beta\sqrt{2}\,\langle\psi_a|\delta(r_A)|\psi_i\rangle \tag{6}$$

and $^3\mathbf{H}$ is the Hessian, *viz.* the A + B matrix of RPA theory, for the triplet manifold, defined as

$$^3\mathbf{H} = (\epsilon_a - \epsilon_i)\delta_{ab}\delta_{ij} - [aj|bi] - [ab|ij] \tag{7}$$

In eq 6 $\{\psi_i\}$ and $\{\psi_a\}$ represent the occupied and virtual (spatial) SCF molecular orbitals of the molecule, with orbital energies ϵ_i and ϵ_a respectively, and the two-electron integrals are written in the charge density notation:

$$[ij|kl] = \int \psi_i^*(1)\psi_j(1)\frac{1}{r_{12}}\psi_k^*(2)\psi_l(2)\,dr_1dr_2 \tag{8}$$

The second-order energy describing the interaction between the nuclear magnetic dipoles is then

$$E_2(A,B) = \mathbf{C}^\dagger(A)\mathbf{V}(B) \tag{9}$$

from which the coupling constant J_{AB} is calculated as

$$J_{AB} = 25982.367 g_A g_B \cdot 2E_2(A,B) \tag{10}$$

where the first numerical constant is a conversion factor so as to yield J_{AB} in hertz. We note that the CPHF method is formally equivalent to the RPA approach and should be closely approximated by the UHF finite perturbation method provided no substantial spin contamination occurs in the UHF calculation.

(35) Andrae, D.; Häussermann, U.; Dolg, M.; Stoll, H.; Preuss, H. *Theor. Chim. Acta* **1990**, *77*, 123.
(36) Igel-Mann, G.; Stoll, H.; Preuss, H. *Mol. Phys.* **1988**, *65*, 1321.
(37) Daoudi, A.; Suard, M.; Barthelat, J. C.; Berthier, G. *J. Mol. Struct.* **1989**, *198*, 215.
(38) Hay, P. J.; Wadt, W. R. *J. Chem. Phys.* **1985**, *82*, 270.
(39) Stevens, W. J.; Krauss, M.; Basch, H.; Jasien, P. G. *Can. J. Chem.* **1992**, *70*, 612.
(40) Huzinaga, S. *J. Chem. Phys.* **1965**, *42*, 1293.
(41) Pople, J. A.; McIver, J. W., Jr.; Ostlund, N. S. *J. Chem. Phys.* **1968**, *49*, 2960.
(42) Pople, J. A.; McIver, J. W., Jr.; Ostlund, N. S. *J. Chem. Phys.* **1968**, *49*, 2965.
(43) Kowalewski, J.; Roos, B.; Siegbahn, P.; Vestin, R. *Chem. Phys.* **1974**, *3*, 70.
(44) Kowalewski, J.; Roos, B.; Siegbahn, P.; Vestin, R. *Chem. Phys.* **1975**, *9*, 29.
(45) Kowalewski, J.; Laaksonen, A.; Roos, B.; Siegbahn, P. *J. Chem. Phys.* **1979**, *71*, 2896.
(46) Sekino, H.; Bartlett, R. J. *J. Chem. Phys.* **1986**, *85*, 3945.
(47) Guest, M. F.; Saunders, V. R.; Overill, R. E. *Mol. Phys.* **1978**, *35*, 427.
(48) Schulman, J. M.; Lee, W. S. *J. Chem. Phys.* **1980**, *73*, 1350.
(49) McCurdy, C. W., Jr.; Rescigno, T. N.; Yeager, D. L.; McKoy, V. In *Modern Theoretical Chemistry*; Schaefer, H. F., III, Ed.; Plenum: New York, 1977; Vol. 3.
(50) Bacskay, G. B. *Chem. Phys.* **1981**, *61*, 385.
(51) Bacskay, G. B. *Aust. J. Phys.* **1982**, *35*, 639.

Table 1. MP2 Energies (E_h) and Equilibrium Bond Lengths (Å) for the $[Os(NH_3)_4L^z(\eta^2\text{-}H_2)]^{(z+2)+}$ Molecular Hydrogen Complexes (Values in Parentheses Are Neutron Diffraction Distances at 165 K and Values in Square Brackets Are X-ray Distances at Liquid Nitrogen Temperature[b] for $[Os(en)_2L^z(\eta^2\text{-}H_2)]^{(z+2)+}$ Complexes)

L^z	E_{MP2}	C_0[c]	r_{HH}[d]	r_{OsH}	r_{OsL^z}	r_{OsN}
$(CH_3)_2CO$	−173.359 95	0.85	1.38	1.59	2.21	2.22
H_2O	−154.213 34	0.88	1.35	1.59	2.20	2.21
CH_3COO^-	−182.264 09	0.84	1.39 (1.34) [1.25]	1.58 (1.60)	2.16 (2.14) [2.15]	2.21 (2.13) [2.12]
Cl^-	−152.410 27	0.88	1.40	1.60	2.55 [2.47]	2.21 [2.15]
H^-	−138.039 40	0.88	1.33	1.63	1.71	2.18
C_5H_5N	−177.917 11	0.82	1.30	1.61	2.28 [2.11]	2.23 [2.12]
CH_3CN	−159.958 12	0.85	1.33	1.58	2.24	2.22

[a] Reference 21. [b] Reference 23. [c] C_0 = coefficient of the SCF reference in normalized MP2 expansion. [d] Calculations at higher levels of correlation suggest that the MP2 H–H distance may be overestimated by ~0.05 Å.

On the other hand, the advantage of the finite field method as used here is that it is readily extended to correlated levels, such as MP2 in a basis of UHF spin orbitals (UMP2), since the quantity of interest is the field dependence of the total energy.

The constrained spatial orbital variation (CSOV) method of Bagus *et al.*[52] has been used to analyze the SCF interaction energy between H_2 and the rest of the Os complex. Denoting these two fragments as A and B with SCF wave functions Ψ_A^0 and Ψ_B^0, respectively, the CSOV analysis starts with the zeroth-order wave function

$$\Psi_{AB}^0 = \hat{A}_{AB}\Psi_A^0\Psi_B^0 \tag{11}$$

i.e. an antisymmetrized product of the fragments' occupied molecular orbitals. The corresponding zeroth-order interaction energy,

$$\Delta E_{AB}^0 = E_{AB}^0 - E_A^0 - E_B^0 \tag{12}$$

where E_A^0, E_B^0, and E_{AB}^0 are the energies corresponding to Ψ_A^0, Ψ_B^0, and Ψ_{AB}^0, respectively, accounts for the electrostatic and Pauli (exchange) repulsion energies between the fragments. Next the wave function Ψ_{AB}^0 is relaxed by successively allowing certain well-defined mixings (rotations) of the orbital spaces, such as o_A/v_A, o_A/v_B, o_B/v_B, and o_B/v_A, where o_A, v_A, o_B, and v_B represent the occupied and virtual orbital spaces of A and B. Full details of the computational aspects of the CSOV method can be found elsewhere.[52,53] The above four mixings are identified as polarization of A, A → B charge transfer, polarization of B, and B → A charge transfer, respectively. As discussed elsewhere,[52,53] the individual polarization and charge transfer energies depend to some extent on the order in which they are calculated. In this work we calculate them in all possible (four) ways and average each type of polarization and charge transfer energy.

The correlation contribution to the interaction energy can be similarly partitioned into intra- and intermolecular terms by expressing the correlation energy in a localized orbital representation. In this work we have used Boys' method of localization.[54] If the correlation energy ϵ can be written in a linear form as

$$\epsilon = \frac{1}{4}\sum_{ij,ab}\langle\Psi_0|H|\Psi_{ij}^{ab}\rangle\, C_{ij}^{ab} \tag{13}$$

$$= \frac{1}{4}\sum_{ij,ab}\langle ij\|ab\rangle\, C_{ij}^{ab} \tag{14}$$

where Ψ_0 and $\{\Psi_{ij}^{ab}\}$ are the SCF reference and all doubly excited Slater determinants, respectively, with coefficients $\{C_{ij}^{ab}\}$ in intermediate normalization, written in terms of the SCF spin orbitals, it can be readily rewritten as

$$\epsilon = \frac{1}{4}\sum_{\mu\nu,ab}\langle\mu\nu\|ab\rangle\{\sum_{ij}C_{ij}^{ab}U_{i\mu}U_{j\nu}\} \tag{15}$$

$$= \frac{1}{4}\sum_{\mu\nu,ab}\langle\mu\nu\|ab\rangle X_{\mu\nu}^{ab} \tag{16}$$

where $\langle ij\|kl\rangle$ is an antisymmetrized electron repulsion integral and U is the unitary matrix that transforms the occupied canonical orbitals $\{\phi_i\}$ to an (orthogonal) localized basis $\{\psi_\mu\}$:

$$\psi_\mu = \sum_i U_{\mu i}\phi_i \tag{17}$$

Therefore the correlation energy can be partitioned into intra- and intermolecular contributions, $\{\epsilon_A\}$ and $\{\epsilon_{AB}\}$, respectively, defined by the equations

$$\epsilon = \frac{1}{4}\sum_A\sum_{\mu\nu\in A}\sum_{ab}\langle\mu\nu\|ab\rangle X_{\mu\nu}^{ab} + \frac{1}{4}\sum_{A\neq B}\sum_{\mu\in A}\sum_{\nu\in B}\sum_{ab}\langle\mu\nu\|ab\rangle X_{\mu\nu}^{ab} \tag{18}$$

$$= \sum_A\epsilon_A + \sum_{A\neq B}\epsilon_{AB} \tag{19}$$

where A and B refer to the appropriate molecular fragments associated with particular subsets of the localized orbitals $\{\psi_\mu\}$. The above equations can be applied to the partitioning of the MP2 as well as CI, averaged coupled pair functional (ACPF),[55] and coupled cluster correlation energies.

As the virtual orbitals are not localized in this scheme, the intra- and intermolecular correlation energies cannot be further decomposed into charge transfer and dipole–dipole contributions.[56] The intramolecular correlation energies do however contain contributions that are regarded as giving rise to basis set superposition effects.[56] The latter are independently estimated, using the counterpoise method of Boys and Bernardi.[57]

Most calculations were performed with the HONDO program,[58] but in some cases (MP3, ACPF, CSOV) the MOLECULE[50,59,60] as well as the TURBOMOLE[61,62] suites of programs were used.

III. Results

A. Geometries. As discussed in section II, the geometries were optimized such that the equilibrium H–H and Os–H distances were determined at the MP2 level with the rest of the geometry optimized at the SCF level. C_s symmetry was assumed in the calculations, with the η^2-H_2 perpendicular to the symmetry plane. The results are summarized in Table 1 which lists the Os–L^z and H–H bond lengths, together with the total MP2 energy.

The Os–N and Os–H distances are remarkably uniform across the seven complexes studied, suggesting that the electronic structures of these compounds are very similar. The variation in the Os–L^z distance is also small for ligands composed of first-row atoms, with a ~0.3 Å increase when Cl^- is the *trans* ligand. The variation in H–H distances is notably small: all distances fall in the range 1.30–1.40 Å. Where comparison with experiment is possible[21,23] we note that agreement between predicted and observed bond lengths is generally good, especially for the H–H

(52) Bagus, P. S.; Hermann, K.; Bauschlicher, C. W. *J. Chem. Phys.* **1984**, *80*, 4378.
(53) Bacskay, G. B.; Kerdraon, D. I.; Hush, N. S. *Chem. Phys.* **1990**, *144*, 53.
(54) Boys, S. F. In *Quantum Theory of Atoms, Molecules and the Solid State: A Tribute to J.C. Slater*; Löwdin, P. O., Ed.; Academic Press: New York, 1966.
(55) Gdanitz, R. J.; Ahlrichs, R. *Chem. Phys. Lett.* **1988**, *143*, 413.
(56) Saebø, S.; Tong, W.; Pulay, P. *J. Chem. Phys.* **1992**, *98*, 2170.
(57) Boys, S. F.; Bernardi, F. *Mol. Phys.* **1970**, *19*, 553.
(58) Dupuis, M.; Rys, J.; King, H. F. *J. Chem. Phys.* **1976**, *65*, 111.
(59) Almlöf, J. MOLECULE USIP report 74-29; Technical report, University of Stockholm, 1974.
(60) Roos, B. O.; Siegbahn, P. E. M. In *Modern Theoretical Chemistry*; Schaefer, H. F., III, Ed.; Plenum: New York, 1977; Vol. 3.
(61) Ahlrichs, R.; Bär, M.; Häser, M.; Horn, H.; Kölmel, C. *Chem. Phys. Lett.* **1989**, *162*, 165.
(62) Häser, M.; Ahlrichs, R. *J. Comput. Chem.* **1989**, *10*, 104.

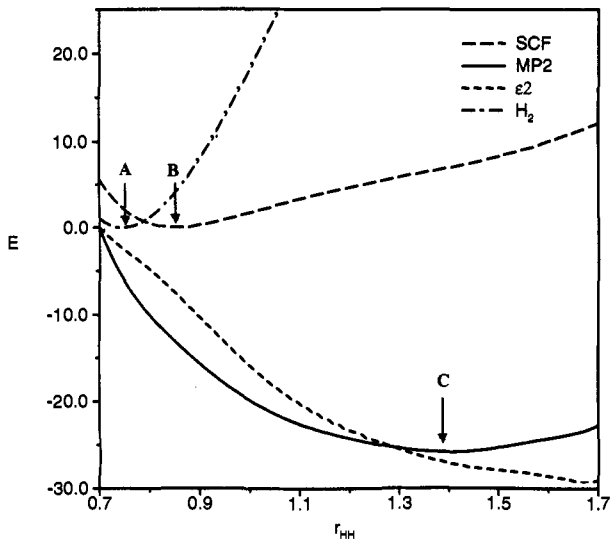

Figure 2. SCF and MP2 energies (kcal/mol) as a function of the H–H distance (Å) for the $[Os(NH_3)_4Cl(\eta^2\text{-}H_2)]^+$ complex. The MP2 curve for H_2 is shown for comparison. The arrows indicate the following: SCF minimum (A), SCF minimum in $[Os(NH_3)_4Cl(\eta^2\text{-}H_2)]^+$ (B), and MP2 minimum for H_2 in $[Os(NH_3)_4Cl(\eta^2\text{-}H_2)]^+$ (C).

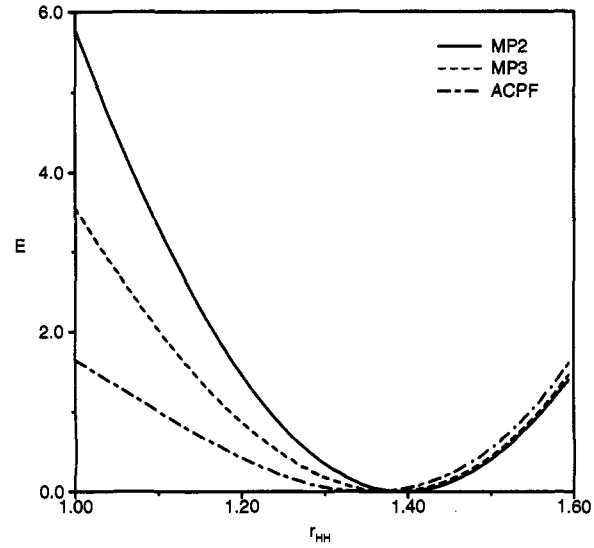

Figure 3. MP2, MP3, and ACPF energies (E_h) as a function of the H–H distance (Å) for the $[Os(NH_3)_4Cl(\eta^2\text{-}H_2)]^+$ complex. (E_{min}(MP2) = −152.41031 E_h, E_{min}(MP3) = −152.43390 E_h, E_{min}(ACPF) = −152.47888 E_h.)

and Os–H distances. The discrepancies in the Os–L^z and Os–N distances are somewhat larger, the maximum being 0.17 Å. These distances were determined at the SCF level and the observed errors are very likely due to the neglect of electron correlation.

For one of the complexes, namely $[Os(NH_3)_4Cl(\eta^2\text{-}H_4)]^+$, the total SCF and MP2 energies as well as the MP2 correlation energy ($\epsilon 2$) are plotted as a function of H–H distance in Figure 2, along with the MP2 curve of H_2 for comparison. It is clear that the large H–H separation is partly due to the extraordinary flatness of the SCF curve. In addition, however, the correlation energy decreases monotonically as the H_2 molecule is stretched. As a result the MP2 curve is also very shallow, with a minimum occurring at 1.4 Å.

A question that needs to be considered is whether a single reference treatment, such as MP2, is valid for the complexes studied here, especially for the prediction of geometries. The coefficient of the SCF reference C_0 in the normalized MP2 wave function (listed in Table 1) is generally ~0.85, which appears somewhat low at first sight. However, this is a result of the very large number of double excitations that enter the wave function with small coefficients ($\leq$0.05). Indeed, if we consider a complex completely dissociated into Os^{2+}, $4NH_3$, L^z, and H_2, the coefficient of the SCF state in each fragment wave function needs to be about 0.97 to yield a value of $0.97^7 \approx 0.85$ for the coefficient of the SCF reference in the MP2 wave function of the completely dissociated complex. Thus there do not appear to be any significant near-degeneracy effects.

The convergence of the perturbation expansion may also be questioned. To test this aspect of the calculations, we carried out MP3 and ACPF[55] calculations at a range of H–H distances. The resulting potential energy curves are depicted in Figure 3, where they are compared with the MP2 curve. (For reasons of clarity, the mimima have been shifted to zero in all cases.) Clearly, the H–H equilibrium distance is only slightly affected on going to a higher level treatment of electron correlation. The MP3 and ACPF H–H bond lengths are 1.38 and 1.35 Å, respectively, somewhat shorter than the MP2 value of 1.40 Å. If a correction of −0.05 Å were applied to the H–H distance in the CH_3COO^- complex, the agreement with the low-temperature neutron diffraction value[22] (1.34 Å) would be even closer. It is likely that in all the other complexes the MP2 H–H distances are also too long by ~0.05 Å in comparison with ACPF. As can be seen in Figures 2 and 3, the potential energy curves have single minima that correspond to a stretched η^2-H_2 complex. No *cis*-dihydrides have been found. This is in contrast with the W complexes studied by Hay,[31] which exhibit well-separated η^2-H_2 and *cis*-dihydride structures, *i.e.* a potential surface with a double minimum, with the η^2-H_2 form being the more stable. In the case of $W(PH_3)_5(\eta^2\text{-}H_2)$, on the other hand, the *cis*-dihydride is the more stable tautomer.

As observed already, C_s symmetry has been assumed in the calculations, so that the ligand L^z would lie in the plane of symmetry with the H_2 molecule perpendicular to it. Such an orientation would be expected to maximize the $\sigma^*(H_2)$–$\pi(L^z)$ interaction through the metal ion. In the case of the C_5H_5N complex, where such an effect might perhaps be expected to be important, the H_2 was also placed parallel to the plane of the symmetry. The resulting H–H distance is however the same as for the perpendicular orientation. This is an indication that for this particular ligand, π interaction has in fact little influence on the H–H bond length. We note, however, that the predicted variation in H–H bond length with L^z is quite small (~0.1 Å). It follows that J_{HD} is *extremely* sensitive to the H_2 bond length at these stretched distances.

Another interesting feature of these Os complexes is that, unlike the compound $W(CO)_3(P^iPr_3)_2(\eta^2\text{-}H_2)$,[3] the most stable structure corresponds to the η^2-H_2 lying between the ligands *i.e.* in a staggered conformation, and not parallel to the N–Os–N axis. In the acetate complex, for example, we find the staggered conformation to be ~2.5 kcal/mol lower in energy than the parallel one, which may be taken as an estimate for the rotational barrier of the η^2-H_2. For $W(CO)_3(PH_3)_2(\eta^2\text{-}H_2)$, on the other hand, we have found the staggered conformation to be 1.3 kcal/mol higher in energy than the parallel structure, when calculated as before at the SCF level.[63]

The Os–H distances also vary very little across this series and are generally in acceptable agreement with the available neutron scattering data.[23,21]

B. Spin–Spin Coupling Constants. Given that the H–D spin–spin coupling constants J_{HD} are expected to correlate with the H–H distance, the experimental coupling constants of the six complexes for which these are available have been plotted against the calculated (MP2) H–H distances, as shown in Figure 4. (The "error bars" indicate that the MP2 distances could be systematically too large by ~0.05 Å, as discussed in section II.) Clearly, there is a reasonable degree of correlation, suggesting that there

(63) Craw, J. S.; Bacskay, G. B.; Hush, N. S. Unpublished results, 1993.

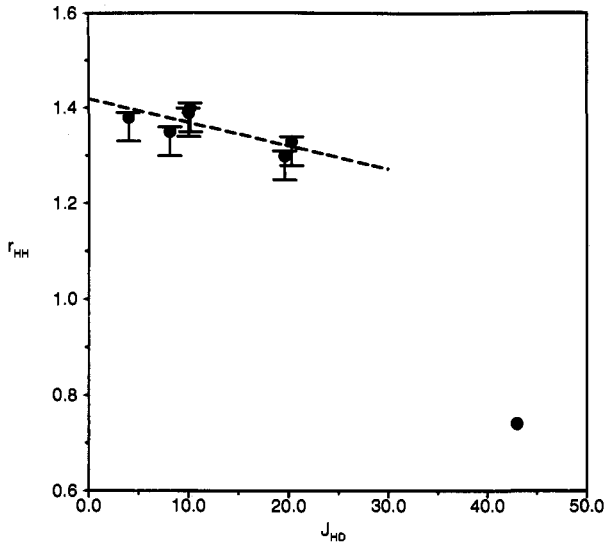

Figure 4. Experimental coupling constant J_{HD} (Hz) versus calculated H–H distance (Å) for the $[Os(NH_3)_4L^z(\eta^2\text{-}H_2)]^{(z+2)+}$ complexes. The point at 43 Hz represents free H_2.

Table 2. Calculated and Experimental Values of the Hydrogen–Deuterium Coupling Constant J_{HD} (Hz)[a] for the $[Os(NH_3)_4L^z(\eta^2\text{-}H_2)]^{(z+2)+}$ Complexes

L^z	J_{HD}(UHF)	J_{HD}(UMP2)	J_{HD}(expt)[b]
$(CH_3)_2CO$	9.3	−2.0	4.0
H_2O	12.2	−4.6	8.1
CH_3COO^-	1.1	8.6	10.0
Cl^-	3.1	6.4	10.2
H^-	2.7	20.9	
C_5H_5N	18.8	−5.8	19.6
CH_3CN	12.0	−2.9	20.3
H_2[c]	54.5	44.6	43.0

[a] Nuclear g values used: 5.5857 (H), 0.8575 (D). [b] Reference 12. [c] Free H_2 value from ref 13.

is an extreme sensitivity of the coupling constant to H–H separation. By comparison, the data of Heinekey and Oldham[19] shows less sensitivity, the slope being more than twice that in Figure 4. Such a distance–coupling constant relationship must therefore be treated with caution, as it is likely to be an empirical observation which at best may be applied to a group of chemically similar compounds, rather than being a universal one. Clearly, free H_2 is very different chemically from complexed H_2 and, as is evident from the data in Figure 4, J_{HD} of free H_2 does not correlate with the J_{HD} of the complexes.

By using finite perturbation theory, as discussed in section II, the Fermi contact contribution to the coupling constant was also calculated, using the UHF and UMP2 formalisms. The results are summarized in Table 2. The underlying assumption in these calculations has been that the orbital and spin–dipole contributions to J_{HD} are likely to be small in comparison with the Fermi contact term, so that a reasonable degree of correlation between calculated and experimental coupling constants might be observed. Unfortunately this does not seem to be the case. On average, the UHF and UMP2 results are in error by ~6 and ~10 Hz, respectively, *i.e.* by an order of magnitude. Accordingly, the correlation between theory and experiment is very tenuous. On the other hand, these computations demonstrate that electron correlation is likely to be an important factor in the accurate prediction of the coupling constant in these complexes and that they are very sensitive to the nature of the complex itself and not likely to depend in a simple way on the H–H distance. This follows from the observation that the Fermi contact contribution to the coupling constant calculated either at the UHF or UMP2 level does not correlate convincingly with the H–H distance, whereas we find that such a treatment appears to be adequate

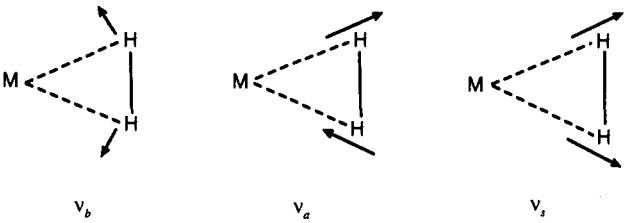

Figure 5. Symmetry coordinates corresponding to the MH_2 vibrations ($M \equiv [Os(NH_3)_4L^z]^{(z+2)+}$).

in the case of free H_2. There is also a strong possibility that in the case of the complexes the level of correlation (UMP2) is insufficient for the calculation of the coupling constant.

The agreement between theory and experiment is much better and certainly more convincing in the case of the H_2 molecule. More extensive studies with successively larger basis sets indicate that a reasonable level of convergence has been reached, even with the DZP basis. Thus *e.g.* use of Dunning's[64] cc-pVPZ *viz.* [5s4p3d2f1g] basis set yields values for the coupling constant of 56.0 and 40.1 Hz at the UHF and UMP2 levels of theory, respectively.

A potential problem with the UHF formalism is that of spin contamination, which in the context of the current calculations means contamination by quintet, septet, *etc.* states. We found however that the coupling constant calculated by the CPHF method is essentially identical with that obtained by the UHF approach; thus spin contamination is not a problem in these complexes.

Nevertheless, in our view, many more detailed and systematic studies are required to arrive at a better understanding and appreciation of the *ab initio* calculation of spin–spin coupling constants and the relative importance of the Fermi contact and dipole–dipole terms. For the time being, for complexes such as those studied here only an order of magnitude prediction of the coupling constant seems possible.

An interesting measure of the interaction of H_2 with the *trans* ligand via the metal complex would be measurement of the spin–spin coupling constant of H (or D) to the *trans* ligand nucleus. The first such measurement for η^2-H_2 complexes has been made by Field *et al.*,[65] who have measured the coupling of ^1H of the η^2-HD to the σ-bound hydride in the Ru complex *trans*-$[RuH(dmpe)_2(\eta^2\text{-}HD)]^+$ (dmpe = 1,2-bis(dimethylphosphino)ethane) to be 4.5 Hz. For the analogous *trans* H–D coupling, this would be 0.7 Hz. We have calculated the coupling between D of η^2-HD and the *trans*-^1H ligand in $[Os(NH_3)_4H(\eta^2\text{-}HD)]^+$ by the finite perturbation method and obtain 2.2 and −2.2 Hz at the UHF and UMP2 levels, respectively. We conclude tentatively that *trans* spin–spin coupling is larger when modulated by the Os(II) "bridge" than by the corresponding Ru(II) moiety.

C. Vibrational Frequencies. The vibrational modes involving the metal atom and the η^2-H_2 part of these complexes can be thought of as those of a triatomic system and can be represented as a symmetric stretch ν_s, an antisymmetric stretch ν_a, and a bend ν_b, as shown in Figure 5. The corresponding force constants are readily calculated by simple finite difference techniques. The resulting harmonic frequencies for the chloride and pyridine complexes are given in Table 3. Os–H_2 stretching vibrational frequencies have been observed for the analogous two ethylenediamine complexes[23] and are in acceptable agreement with the calculated harmonic frequencies ν_s and ν_a, considering the inherent limitations of the calculations, *viz.* use of a harmonic model and the neglect of the metal fragment's (intramolecular) modes. The error in the calculated frequencies is estimated as ~10%. Thus, the small difference in the observed frequencies (Table 3) would

(64) Dunning, T. H., Jr. *J. Chem. Phys.* **1989**, *90*, 1007.
(65) Field, L. D.; Hambley, T. W.; Yau, B. C. K. *Inorg. Chem.* **1994**, in press.

Table 3. MP2 Force Constants (au) and Harmonic Vibrational Frequencies (cm^{-1}) for the $[Os(NH_3)_4L^z(\eta^2\text{-}H_2)]^{(z+2)+}$ Complexes[a]

L^z	f_s	f_a	f_b	f_{sb}	ν_b	ν_a	ν_s	ν_{expt}[b]
Cl^-	0.207	0.208	0.085	0.020	1318	2335	2358	2155
C_5H_5N	0.190	0.203	0.094	0.042	1283	2310	2305	2285

[a] s = symmetric stretch, a = asymmetric stretch, b = bend. The expected error in the calculated frequency is ~10%. s = [b] Reference 23.

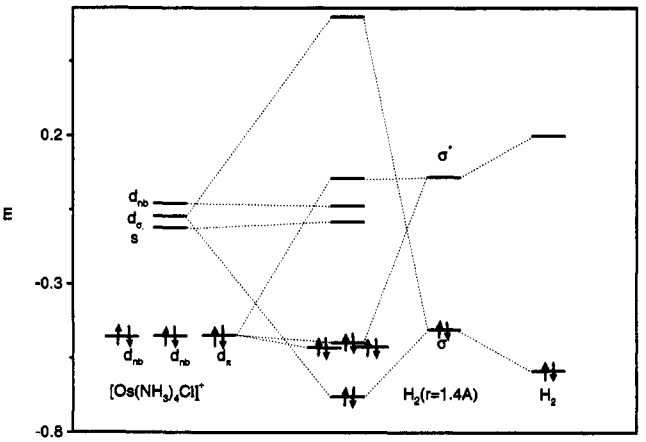

Figure 6. Orbital energy level diagram (E_h) for the $[Os(NH_3)_4Cl]^+$ fragment interacting with H_2.

not be expected to be reproduced, given the anticipated accuracy of the calculations. The effective mass used for the metal fragment has negligible effect on the calculated frequencies, as the reduced mass of a given mode is dominated by that of H_2. The stretching frequencies are fairly typical of hydride modes; for example the calculated[66] fundamental frequency in the ground state of osmium monohydride ($^4\Pi$) is 2138 cm^{-1}, within 200 cm^{-1} of those of the complexes (Table 3). The bending mode ν_b, which can be thought of as an H_2 stretch, is about one-third of the calculated MP2 stretching frequency of 4680 cm^{-1} of free H_2 or indeed of the corresponding experimental frequency of 4401 cm^{-1}. The similarity between the vibrational frequencies in the two complexes suggests a similar degree of bonding and H–H distances, as found.

By comparison, in $W(CO)_3(P^iPr_3)_2(\eta^2\text{-}H_2)$[4] the H_2 stretching frequency is considerably higher at ~2700 cm^{-1}, while the W–H_2 frequencies at 1570 and 953 cm^{-1} are lower. Thus the Os–H bond in these complexes appears to be considerably stronger than the W–H bond in the above complex, as expected, since formally Os is dipositive in these complexes, whereas W is neutral. Note however that the Fe(II) η^2-H_2 complex is known to be weakly bound, with a "normal" H_2 distance, since for this complex the π donation is probably much smaller from the tightly bound 3d orbitals than from the comparatively diffuse 5d orbitals of Os.

D. Charge Distribution and Bonding. An orbital energy level diagram illustrating the major types of orbital interactions (mixings) between the $[Os(NH_3)_4Cl]^+$ and H_2 fragments is given in Figure 6. The important features are, firstly, that on stretching the H_2 bond the σ level rises in energy, moving closer to the d_σ Os orbital, so that orbital delocalization, *i.e.* charge donation, becomes more favorable. At the same time the σ^* orbital of H_2 drops in energy, which facilitates its mixing with the d_π occupied Os orbital, hence a greater degree of back-donation can occur. The other Os d orbitals play little role in the bonding, their energies hardly changing as the η^2-H_2 complex forms; they are thus designated d_{nb} (nonbonding).

Although the diagram in Figure 6 is for the chloride complex, no qualitative difference is observed as the L^z ligand is changed. We may expect that a reasonable amount of charge redistribution will occur as the complex forms; population analyses to test this have been carried out on all the complexes using the Roby–Davidson[67-70] as well the as the Mulliken method.[71]

The atomic charges calculated by the Roby–Davidson method are listed in Table 4. We note that these appear generally to be chemically "sensible", *i.e.* they are qualitatively those that might be expected on the basis of formal oxidation states. Thus the Os charge in all cases except for $L^z = H^-$ (where it is 0.44) is greater than 1, compared with a formal charge of 2. Such values appear considerably more reasonable than the unphysical negative charges reported by Maseras and Morokuma[72] with use of the Mulliken and the "natural" population analysis[73] for $[Os(PH_3)_4(H)(\eta^2\text{-}H_2)]^+$.

An important feature of the Roby–Davidson charge distributions is that the net charge on H_2 shows little variation with the ligand L^z. In the case of neutral ligands H_2 carries a small positive charge but becomes negative (indicating excess electrons) for the negatively charged ligands. The removal of H_2 from the complex makes the Os atom more positive, except in the case of the charged ligands, where the opposite happens. The change in the Os charge is to a large extent counterbalanced by a corresponding change, in the opposite direction, in the charge on the ligand L^z. The shared electron number η of H_2 ranges from 0.27 to 0.40, and thus indicates a significant degree of bonding between the two H atoms, although this bond is considerably weaker than in free H_2 where $\eta = 1.44$, or even in free stretched H_2 with $\eta = 0.88$. The Os–H shared electron numbers are ~0.9, implying a strong bond, as expected on the basis of the short Os–H distances (Table 1). The three center shared electron terms η(HOsH) and η(HOsL^z) are small but not insignificant, indicating that the bonding cannot be described completely by two center terms.

For comparison, the Mulliken charges for the complexes and the fragments, as well as the bond indicies, as defined by Villar and Dupuis,[74] are given in Table 5. The Mulliken charges, although qualitatively different from those obtained by the Roby–Davidson method, display similar trends. The most significant difference is that the Os charges are much lower when calculated by the Mulliken method. The charged L^z ligands are less negative while the ammonias are more positive. The bond indicies are consistent with a strong Os–H bond and a fairly weak H_2 bond.

In Table 6 a partitioning of the differences in the Mulliken gross electron populations of the $[Os(NH_3)_4L^z(\eta^2\text{-}H_2)]^{(z+2)+}$ complex and of the $[Os(NH_3)_4L^z]$ and the H_2 fragments into σ and π contributions is presented. The orbitals are characterized as σ or π depending on whether they can interact (mix) with the σ or σ^* orbitals of H_2. Thus the charge transfer can be monitored orbital by orbital. The σ donation from H_2 into the metal d_σ is clearly very large, but the back-donation into the σ^* orbital of H_2 almost matches this, resulting in H_2 being positive overall. In comparison with H_2 and Os, L^z hardly participates in the charge transfer.

As a final illustration of the charge transfer effects, the electron density difference between the complex $[Os(NH_3)_4Cl(\eta^2\text{-}H_2)]^+$ and its constituent fragments $[Os(NH_3)_4Cl]^+$ and (stretched) H_2 is plotted, as shown in Figure 7. The densities were calculated in a plane perpendicular to the C_s (xy) plane, *viz.*

$$\rho = |\Psi(x,0,z)|^2 \qquad (20)$$

where Ψ is the molecular wave function and ρ the corresponding electron density function. A buildup of charge on H_2 is evident, together with a charge buildup and depletion around the Os, consistent with electron donation from the d_π orbital. A hardly perceptible density change occurs around Cl^-, the L^z ligand. Very

(66) Benavides-Garcia, M.; Balasubramanian, K. *J. Mol. Spectrosc.* **1991**, *150*, 271.
(67) Davidson, E. R. *J. Chem. Phys.* **1967**, *46*, 3320.
(68) Roby, K. R. *Mol. Phys.* **1974**, *27*, 81.
(69) Heinzmann, R.; Ahlrichs, R. *Theor. Chim. Acta* **1976**, *42*, 33.
(70) Ehrhardt, C.; Ahlrichs, R. *Theor. Chim. Acta* **1985**, *68*, 231.
(71) Mulliken, R. S. *J. Chem. Phys.* **1955**, *23*, 1833.
(72) Maseras, F.; Morokuma, K. *Chem. Phys. Lett.* **1992**, *195*, 500.
(73) Reed, A. E.; Curtiss, L. A.; Weinhold, F. *Chem. Rev.* **1988**, *88*, 899.
(74) Villar, H. O.; Dupuis, M. *Chem. Phys. Lett.* **1987**, *142*, 59.

Table 4. Roby–Davidson Population Analysis: Charges (e) and Two- and Three-Center Shared Electron Numbers η for the $[Os(NH_3)_4L^z(\eta^2\text{-}H_2)]^{(z+2)+}$ Complexes (Results for Complex without the η^2-H_2 Are Given in Parentheses

L^z	$q(H_2)$	$q(Os)$	$q(L^z)$	$q(NH_3)$	$\eta(H_2)$	$\eta(HOs)$	$\eta(HOsH)$
$(CH_3)_2CO$	0.10	1.23 (1.55)	0.13 (0.02)	0.14 (0.11)	0.39	0.85	0.14
H_2O	0.10	1.24 (1.53)	0.06 (0.02)	0.15 (0.11)	0.30	0.94	0.17
CH_3COO^-	–0.07	1.36 (1.24)	–0.81 (–0.74)	0.13 (0.13)	0.27	0.84	0.07
Cl^-	–0.08	1.26 (1.00)	–0.71 (–0.41)	0.14 (0.10)	0.28	0.76	0.05
H^-	0.03	0.44 (0.70)	–0.06 (–0.02)	0.15 (0.17)	0.36	1.02	0.24
C_5H_5N	0.06	1.26 (1.26)	0.18 (0.17)	0.13 (0.14)	0.40	0.87	0.17
CH_3CN	0.06	1.27 (1.21)	0.08 (0.03)	0.15 (0.19)	0.31	0.90	0.15

Table 5. Mulliken Population Analysis: Charges (e) and Bond Indices P for the $[Os(NH_3)_4L^z(\eta^2\text{-}H_2)]^{(z+2)+}$ Complexes (Results for Complex without the η^2-H_2 Are Given in Parentheses)

L^z	$q(H_2)$	$q(Os)$	$q(L^z)$	$q(NH_3)$	$P(H_2)$	$P(HOs)$
$(CH_3)_2CO$	0.16	0.49 (0.76)	0.14 (0.15)	0.30 (0.27)	0.15	0.85
H_2O	0.22	0.37 (0.73)	0.15 (0.18)	0.31 (0.27)	0.17	0.83
CH_3COO^-	0.07	0.41 (0.59)	–0.64 (–0.61)	0.29 (0.26)	0.15	0.84
Cl^-	0.08	0.13 (0.32)	–0.44 (–0.38)	0.31 (0.27)	0.15	0.83
H^-	0.00	0.04 (0.16)	–0.19 (–0.09)	0.29 (0.23)	0.21	0.78
C_5H_5N	0.19	0.42 (0.71)	0.18 (0.22)	0.30 (0.27)	0.22	0.83
CH_3CN	0.18	0.46 (0.79)	0.13 (0.11)	0.31 (0.27)	0.18	0.81

Table 6. Mulliken Population Analysis: Partitioning of the Difference in Gross Populations (e) between the $[Os(NH_3)_4L^z(\eta^2\text{-}H_2)]^{(z+2)+}$ Complex and the Fragments $[Os(NH_3)_4L^z]^{(z+2)+}$ and H_2 into σ and π Contributions

	$q(H_2)$		$q(Os)$		$q(L^z)$	
L^z	σ	σ^*	σ	π	σ	π
$(CH_3)_2CO$	–0.61	0.45	0.64	–0.36	0.01	–0.01
H_2O	–0.70	0.48	0.74	–0.37	0.03	–0.01
CH_3COO^-	–0.65	0.58	0.65	–0.46	0.04	–0.01
Cl^-	–0.65	0.56	0.66	–0.45	0.07	–0.01
H^-	–0.53	0.53	0.51	–0.40	0.09	0.00
C_5H_5N	–0.67	0.48	0.78	–0.36	–0.10	0.04
CH_3CN	–0.67	0.49	0.70	–0.37	0.10	–0.03

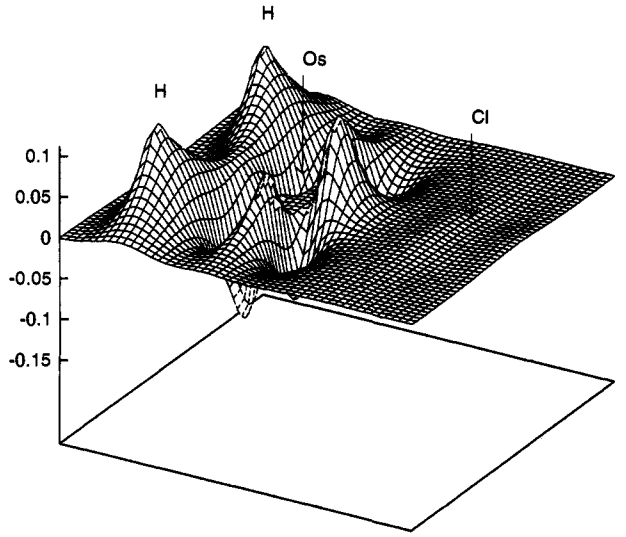

Figure 7. Density difference plot of $[Os(NH_3)_4Cl(\eta^2\text{-}H_2)]^+$–$[Os(NH_3)_4Cl]^+$–$H_2$.

similar plots were obtained for several other complexes too, suggesting that H_2 becomes uniformly negative. This appears to be contradictory to the Mulliken populations, as well as, in some instances, the Roby–Davidson charges. We note, however, that the densities implicit in these plots are not integrated densities and thus the degree of charge transfer may appear somewhat exaggerated. The main reason for the discrepancy is however the non-zero population in the Os 6s and 6p orbitals. Being fairly diffuse, they make a considerable contribution to the electron density in the region occupied by H_2, especially since the Os–H_2 distances are quite small. In the population analyses such

Table 7. MP2 Binding Energies ΔE_B and Their Correlation Components $\Delta\epsilon$ (kcal/mol) for the $[Os(NH_3)_4L^z(\eta\text{-}H_2)]^{(z+2)+}$ Complexes

L^z	ΔE_B	$\Delta\epsilon$	L^z	ΔE_B	$\Delta\epsilon$
$(CH_3)_2CO$	–64.0	–47.4	H^-	–40.2	–44.3
H_2O	–57.7	–51.5	C_5H_5N	–46.7	–40.5
CH_3COO^-	–59.0	–43.0	CH_3CN	–49.3	–41.5
Cl^-	–60.8	–44.5			

contributions show up as overlap and shared electron terms in the Mulliken and Roby–Davidson analyses, respectively. Such terms are equally divided between a given pair of atoms; that is quite arbitrary and has been long recognized as a weakness of the population analyses. Unfortunately, quantum mechanics does not allow for the rigorous and unambiguous definition of chemical concepts such as atomic charge. We note however that the method developed by Bader[75] and co-workers, where atomic charges are obtained on the basis of spatial topology, would probably yield charges in qualitative agreement with our density difference map, *i.e.* would predict H_2 to be slightly negative in the Os complexes.

The binding energies, *i.e.* energies associated with the reactions,

$$[Os(NH_3)_4L^z](eq) + H_2(eq) \xrightarrow{\Delta E_B} [Os(NH_3)_4L^z(\eta^2\text{-}H_2)](eq) \quad (21)$$

calculated at the MP2 level, are given in Table 7. The reactant and product energies that yield ΔE_B were computed at their respective equilibrium geometries (consistent with the method of geometry optimization used). Clearly, the bond between Os and H_2 is very strong in these complexes, which is largely a consequence of the unique type of electron correlation found in these systems. Moreover, as shown in Figure 8, the calculated binding energies correlate reasonably well with the H–H distances. Although the σ donation and σ^* back-bonding model is effectively a one-electron description of the bonding, it is interesting that it is the total binding energy that correlates with H–H distance.

A more detailed analysis of the bonding has been carried out for the chloride system that will now be discussed. The energies associated with the formation of $[Os(NH_3)_4Cl(\eta^2\text{-}H_2)]^+$ from $[Os(NH_3)_4Cl]^+$ and H_2 have been analyzed first at the SCF level using the CSOV technique followed by an analysis of the correlation contributions calculated at the MP2 level. Given that the H–H equilibrium distance in the η^2-H_2 complex is very different from the free H_2 value, the energetics associated with the reaction,

(75) Bader, R. F. W. *Atoms in Molecules: A Quantum Theory*; Clarendon Press: Oxford, 1990.

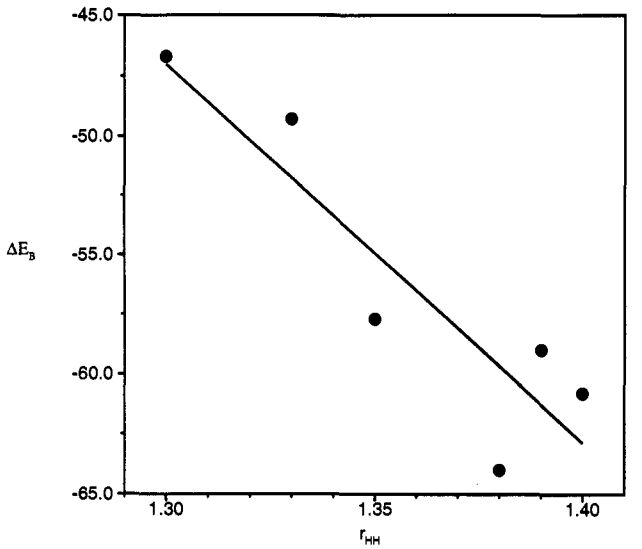

Figure 8. Binding energy, ΔE_B (kcal/mol), versus H–H distance (Å) for the $[Os(NH_3)_4L^z(\eta^2\text{-}H_2)]^{(z+2)+}$ complexes.

Table 8. Analysis of the SCF and MP2 Correlation Components of the Interaction Energy between $[Os(NH_3)_4Cl]^+$ (≡MX) and H_2 at the MP2 Equilibrium Geometry of $[Os(NH_3)_4Cl(\eta^2\text{-}H_2)]^+$ and the Energetics of Geometry Relaxations of MX and H_2 (kcal/mol)

energy contribution	ΔE_{SCF}	$\Delta\epsilon_{MP2}$
electrostatic + repulsion	158.3	
MX polarization	–40.7	
H_2 polarization	–20.8	
$H_2 \rightarrow$ MX charge transfer	–132.2	
MX $\rightarrow H_2$ charge transfer	–52.8	
H_2 intramolecular correlation		10.6
MX intramolecular correlation		–20.5
MXη^2-H_2 intermolecular correlation		–29.5
total	–88.3	–39.5
$H_2(eq) \rightarrow H_2(*)$	67.9	–4.4
$MX(eq) \rightarrow MX(*)$	4.1	–0.6
$MX(eq) + H_2(eq) + \Delta E \rightarrow MX(\eta^2\text{-}H_2)$[a]	–16.3	–44.5

[a] Association energy relative to MX and H_2 with all species at their equilibrium geometries.

$$MX(eq) + H_2(eq) \xrightarrow{\Delta E} MX(\eta^2\text{-}H_2)(eq) \qquad (22)$$

where MX denotes $[Os(NH_3)_4Cl]^+$ and all species are at their respective equilibrium (eq) geometries, could be analyzed in two distinct ways, as summarized by the following reactions:

(a)
$$MX(eq) + H_2(eq) \xrightarrow{\Delta E_1} MX(*) + H_2(*) \qquad (23)$$

$$MX(*) + H_2(*) \xrightarrow{\Delta E_2} MX(\eta^2\text{-}H_2)(eq) \qquad (24)$$

(b)
$$MX(eq) + H_2(eq) \xrightarrow{\Delta E_1'} MX(\eta^2\text{-}H_2)(\dagger) \qquad (25)$$

$$MX(\eta^2\text{-}H_2)(\dagger) \xrightarrow{\Delta E_2'} MX(\eta^2\text{-}H_2)(eq) \qquad (26)$$

where MX(*) and H_2(*) denote MX and H_2 at the geometries these species assume in MXη^2-H_2(eq), while in MX$(\eta^2$-$H_2)(\dagger)$ the MX and H_2 fragment geometries are constrained at their free equilibrium values. The total association energy corresponding to process 22 is of course

$$\Delta E = \Delta E_1 + \Delta E_2 = \Delta E_1' + \Delta E_2' \qquad (27)$$

The results of the analysis according to Scheme a (reactions 23 and 24) are given in Table 8. Starting at the geometry specific to the MX$(\eta^2$-$H_2)$ complex we note that a large stabilization is predicted at the SCF level, *viz.* –88.3 kcal/mol, that is dominated by the charge transfer contributions, i.e. the mixing of occupied orbitals of H_2 with unoccupied orbitals of MX and *vice versa*. The attractive charge transfer and polarization terms more than compensate for the repulsion due to the overlap of the doubly occupied orbitals. The MP2 correlation energy has been decomposed into intra- and intermolecular contributions; the results indicate that the H_2 intramolecular term is repulsive, *i.e.* there is a loss of correlation in the H_2 fragment as the complex forms, but the MX intramolecular as well as the intermolecular terms are strongly attractive and the resulting stabilization due to electron correlation, –39.5 kcal/mol, is about one-third of the total, ΔE_2 ($=\Delta E_{SCF} + \Delta\epsilon_{MP2}$) = –127.8 kcal/mol. However, when the total association (binding) energy ΔE is to be calculated relative to MX and H_2 at their equilibrium geometries, the changes in (intramolecular) geometries need to be taken into account, as indicated by eq 27. The energy ΔE_1 of the latter process is 67 kcal/mol, largely due to the stretching of the H_2 bond. Consequently, the net association energy ΔE is –60.8 kcal/mol. Although this energy appears to be dominated by the correlation component, *viz.* –44.5 kcal/mol, the above analysis shows that it is in fact due to a near cancellation of the SCF components of ΔE_1 and ΔE_2. Correction for basis set superposition effects by the counterpoise method[57] reduces the magnitude of the association energy by 10.6 kcal/mol. The bulk of the correction is to the correlation energy. The corrected H_2 and MX intramolecular correlation energies are 12.0 and –12.7 kcal/mol, respectively. Such corrections, while important in the quantitative description of bonding, do not alter any of our qualitative conclusions.

As noted in section II, the CSOV results quoted are the averages of results that were obtained in four separate calculations that differ in the order of the various orbital relaxations. Due to the non-orthogonality of the fragments' molecular orbitals the individual estimates of polarization and charge transfer energies vary, which can also be interpreted in terms of synergistic couplings.[77] In the present case, specifically for the data in Table 8, the variations are relatively large: approximately 11%, 19%, and 12% in the $H_2 \rightarrow$ MX and MX $\rightarrow H_2$ charge transfer and MX polarization terms, respectively, but 100% in the case of the H_2 polarization. The large variation in the H_2 polarization estimates is a consequence of the substantial overlap between the H_2 and MX virtual orbitals and the very large $H_2 \rightarrow$ MX charge transfer energy. Thus, if H_2 polarization is allowed for prior to the $H_2 \rightarrow$ MX charge transfer, the drop in energy is twice as large as that obtained when the order of calculations is reversed. In the former case polarization is overestimated as it is likely to contain part of the $H_2 \rightarrow$ MX charge transfer energy. We emphasize that the CSOV analysis provides a useful, qualitative guide to the bonding mechanism, but the individual contributions to the binding energy are not quantities that can be rigorously defined and calculated, as noted elsewhere already.[52,53,76] As expected, however, the synergistic couplings fall off sharply with MX–H_2 distance.

A CSOV analysis has been performed at the SCF equilibrium geometry of the Cl^- complex as well, where the H_2 bond length is 0.85 Å and the Os–H distance is 1.72 Å. To test the sensitivity of the results to the latter parameter, the analysis was repeated at the MP2 Os–H_2 separation of 1.54 Å. This last calculation effectively corresponds to Scheme b (eqs 25 and 26), outlined above, since the $[Os(NH_3)_4Cl]^+$ and H_2 geometries are very close to their respective equilibrium geometries. The results are summarized in Table 9.

Comparison of the three sets of CSOV results in Tables 8 and 9 shows that when H_2 is stretched the charge transfer energies become dramatically larger. The polarization contributions also become more significant, so the two attractive components of the

(76) Frey, R. F.; Davidson, E. R. *J. Chem. Phys.* **1989**, *90*, 5555.
(77) Pacchioni, G.; Bagus, P. S. *Inorg. Chem.* **1992**, *31*, 4391.

Table 9. CSOV Analysis of the SCF Interaction Energy (kcal/mol) between $[Os(NH_3)_4Cl]^+$ (≡MX) and H_2 at the SCF Equilibrium Geometry at Different Os–H_2 Separations (Å)

	r_{Os-H_2}	
energy contribution	1.72	1.54
electrostatic + repulsion	55.2	101.5
MX polarization	−9.1	−14.3
H_2 polarization	−8.4	−13.2
$H_2 \rightarrow$ MX charge transfer	−51.9	−76.8
MX $\rightarrow H_2$ charge transfer	−14.3	−22.4
total (SCF)	−28.5	−25.1

SCF energy more than compensate for a large fraction of the increased repulsion, resulting in a very flat potential energy curve, as seen in Figure 2. The results are less sensitive to the change in the Os–H distance. However as noted already, electron correlation also favors a larger H–H separation.

The CSOV results suggest that energetically the $H_2 \rightarrow$ Os σ donation is ca. 2.5 times as important as the π back-donation, while on the basis of the population analyses these two terms may be expected to be comparable. This apparent contradiction may be due to different energetic contributions of the two types of charge flow or to possible inaccuracies in the population analyses, or it may result from the calculated charge differences implicitly including the charge redistribution that results from the orthogonalization of the fragments' orbitals that occurs as interaction is allowed for. The energetic effects of the latter are included in the electrostatic + repulsion term rather than in the CSOV charge transfer energies. We plan to investigate these ideas in detail in the near future. The charge flow could also be quantified by monitoring the variation of the dipole moment that occurs as the CSOV calculation proceeds.[77] Unfortunately, for the chloride complex at its equilibrium geometry the dipole moment appears to be far too sensitive to the order of orbital relaxations in the CSOV scheme to allow a sensible conclusion to be reached.

In summary, stretching of H_2 enhances charge transfer and polarization although at the SCF level they are more than cancelled by the energy loss associated with the pure stretching process. As correlation also favors the stretched geometry, the result is a large H–H separation with a large correlation contribution to the binding energy. We note, however, that if we compare the SCF and MP2 binding energies calculated with the appropriate SCF and MP2 optimized geometries, the SCF energy of −28.5 kcal/mol is approximately half of the MP2 value of −60.8 kcal/mol.

IV. Discussion and Conclusions

Dissociative uptake of dihydrogen, the simplest molecule, by metal complexes leading to formation of dihydrides by oxidative addition has been studied extensively, but the relatively new discovery of molecular binding of H_2 raises interesting new problems of interpretation in terms of electronic structure. A characteristic feature of the W complexes, which were the first to be studied both experimentally and theoretically,[1-4] is the coexistence of stable forms of undissociated (η^2-H_2) and dissociated dihydride tautomers. Our theoretical investigation of the Os(II) complexes of Li and Taube[12] reveals that these represent a new class of structures in which there is only one stable form, corresponding to a single non-dihydride minimum on the potential energy surface. This basic structural difference is a consequence of the very much larger ligand binding energy ΔE_B of the Os(II) species, predicted to be in the range −40 to −64 kcal/mol, as compared with values of the order of −10 kcal/mol for the W complexes. This can be qualitatively understood in terms of the potential energy diagrams shown in Figure 9. The left-hand curves (I) represent the potential energy of H–H stretching in a hypothetical structure consisting of an intact H_2 interacting weakly with an Os moiety, with equilibrium H–H distance equal to that of free H_2 (0.74 Å), while the right-hand diabatic curves (II) represent the potential energy for the corresponding stretch in a dihydride, with equilibrium H–H separation characteristic of these species (*ca.* 1.8 Å). Three possibilities are illustrated. In Figure 9, parts A and B, respectively, the minima of the diabatic curves are close in energy, with only weak electronic coupling, that leads to an avoided crossing, and hence to a low binding energy with a double potential minimum. Figure 9A, in which the η^2-H_2 form is energetically preferred, is thus characteristic of complexes such as $W(CO)_3(PH_3)_2(\eta^2\text{-}H_2)$, while Figure 9B, in which the dihydride tautomer is preferred, is characteristic of complexes such as $W(PH_3)_5(\eta^2\text{-}H_2)$, according to the calculations of Hay.[31] Figure 9C represents the new situation exemplified by the Os(II) complexes: very strong coupling at the crossing point, leading to a single-minimum surface with an equilibrium H–H distance very different from that of the diabatic curves, and hence to a large binding energy. Both of these features are predicted for the Os(II) species, the H–H bond lengths calculated to be in the range 1.3–1.4 Å clearly meriting the description of "stretched" H_2 complexes.[12] Further lowering of curve II with respect to curve I, with increased coupling, will lead ultimately to a single-minimum dihydride description. The existence of a single minimum resembles to some extent the situation e.g. in organometallic complexes of substituted silanes that have been described in terms of M–Si–H three-center bonds.[78,79]

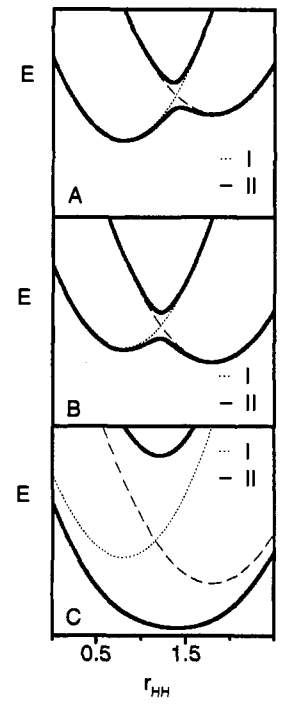

Figure 9. Schematic potential energy relationships. The left (I) and right-hand (II) curves represent the potential energy of H–H stretching in a hypothetical structure consisting of an intact H_2 interacting with an Os moiety and in a *cis*-dihydride, respectively. A and B correspond to small electronic coupling, thus both tautomers may exist, whereas C represents strong coupling leading to a stretched η^2-H_2 complex.

The basic nature of the intact dihydrogen–metal complex bond in all known species appears to be of the same kind as that originally proposed for the bond between metal ions and olefins in π-complexes[33,34]—*i.e.*, electron donation to the metal complex from the H_2 σ-orbital, accompanied by π back-bonding which provides additional stabilization, both leading to an increase in the H–H equilibrium bond length. This is quantified for the

(78) Rabaâ, H.; Saillard, J.-Y.; Schubert, U. *J. Organomet. Chem.* **1987**, *330*, 397.
(79) Lichtenberger, D.; Rai-Chaudhuri, A. *Inorg. Chem.* **1990**, *29*, 975.

Os(II) species at the SCF level in the Mulliken population analyses in Table 6, which show 61–70% σ donation away from the H_2 (somewhat less for the H^- complex) and 45–58% π back-donation into the corresponding σ^* orbital. Thus the overall picture corresponds to a well-established model. However, detailed analysis does not yield a simply-interpretable quantitative understanding of the modulation of properties of the complexes by variation of the ligand L^z, which is the most interesting feature of these complexes.

The first important theoretical point revealed by the quantum calculations is the critical importance of electron correlation, *i.e.* the inadequacy of a description in terms of a single configuration wave function. This has a larger effect on the predicted H–H distances (*ca.* 60%) than hitherto found for any other molecule, resulting, in the present case, from the extraordinary flatness of the potential surface. Similarly, the correlation contribution to the binding energies is also unusually large. Detailed understanding of the modulation of properties as the *trans* ligand L^z is varied therefore requires a knowledge of the intra- and intermolecular correlation contributions as well as the individual SCF (electrostatic, charge transfer, *etc.*) terms. However, it is useful when considering these molecules, to look for some general trends, both within the theoretical predictions and also with experimental quantities.

We have already noted (Figure 8) the approximately linear correlation between predicted H–H bond length and binding energy ΔE_B, the larger binding energies being associated with longer bond distances. A physical property of much practical interest is the spin–spin coupling constant. We have noted that while *ab initio* calculations (which appear to be the first attempted for metal complexes) yield values of the same order of magnitude as the experimental ones, much further work will be necessary to achieve quantitative consistency between theory and experiment. However, it is useful to note correlation of the experimental values of J_{HD} with other properties. The quasilinear correlation of J_{HD} with predicted bond length (with a gradient *ca.* twice that proposed[19] for η^2-H_2 complexes with shorter H–H distances) has been demonstrated in Figure 4. It follows that there is also a near-linear correlation of J_{HD} with binding energy ΔE_B. It should perhaps be mentioned that there is a reasonable degree of correlation between J_{HD} and the square of the bond index $P(H_2)$ (Table 5), similar to that frequently employed in discussions of spin–spin coupling constants in unsaturated and aromatic hydrocarbons.[80] However, the significance of this is probably the relation of bond index to bond length rather than conformity to the simplified "average energy" SCF approximation embodied in the earlier analysis of coupling constants.[80]

Finally, we note that the analyses of electronic structures do not immediately reveal close connections with the chemical nature of the *trans* ligands L^z. In order to get some feel for this, and perhaps suggest qualitative predictions of properties of complexes not yet synthesized, we offer a simple qualitative model where we greatly simplfiy the H_2 interaction with the complex $[Os(NH_3)_4L^z]^{(z+2)+}$ according to the scheme shown in Figure 6 and consider only the location and separation Δ of the Os d_σ and d_π levels and those of the H_2 σ and σ^* orbitals. The degree of interaction will primarily be a function of (i) Δ and (ii) the separation of centers of gravity of the Os and H_2 levels, respectively.

Since the Os d levels of interest lie in the (stretched) σ–$\sigma^*(H_2)$ energy interval, interaction leading to η^2-H_2 bond formation will be favored by raising the level of d_π and/or lowering d_σ, *i.e.* by decreasing Δ. Thus effect (i), together with the previously mentioned regularities, implies the following: (A) A small value of Δ is anticipated to be associated with strong interaction, large binding energy ΔE_B, small spin–spin coupling constant J_{HD}, and relatively large H–H separation. (B) Conversely, a large value of Δ will be expected to be linked to strong interaction, smaller binding energy ΔE_B, larger J_{HD}, and smaller H–H separation. Experimentally, in the field of transition metal complex spectroscopy, the separation $\Delta(L)$ for a ligand L is, for a given metal, essentially a linear function of the spectrochemical parameter $f(L)$.[81] Thus, for approximately constant relative centers of gravity of Os and H_2 levels, the above trends would imply small $f(L) \rightarrow$ small Δ, with consequences A, or large $f(L) \rightarrow$ large Δ, with consequences B.

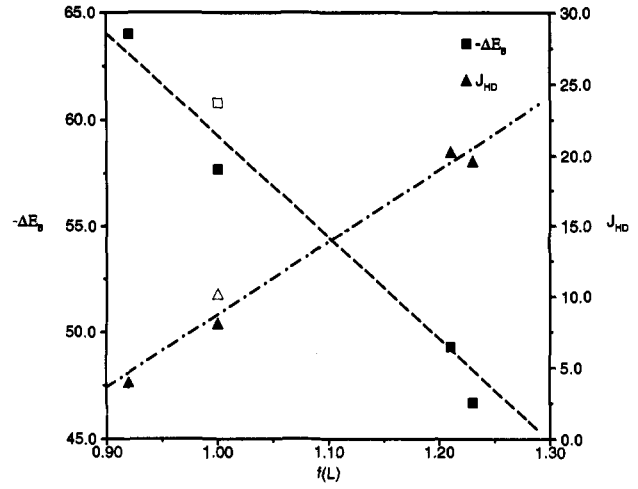

Figure 10. Correlation of binding energy ΔE_B (kcal/mol) and spin–spin coupling constant J_{HD} (Hz) with spectrochemical parameter $f(L)$. The open symbols (□, △) correspond to the modified parameter $f^*(L)$ for the (charged) Cl^- anion (see text).

According to the angular overlap (AO) model[82] Δ can be written as

$$\Delta = 3e_\sigma - 4e_\pi \qquad (28)$$

where e_σ and e_π are measures of σ-donor and π-acceptor capacities respectively. In this formalism e_σ is always positive. The value of e_π is positive for ligands with moderately large *π-donor* character (*e.g.* halides) and negative for those with strong *π-acceptor* character (*e.g.* acetonitrile). Other things being equal, these result in low and high values of $f(L)$, respectively.

The second effect mentioned above is the position of the center of gravity of the relevant Os d levels; for negatively charged ligands (*e.g.* Cl^-), these will be raised relative to those with neutral L. This will increase the d–σ^* separation. If the π-donor character of the ligand L is dominant in the interaction, the binding will be stronger for equivalent values of Δ when the ligand is negatively charged. Thus an "effective" spectrochemical parameter $f^*(L)$ could be introduced in this context, where $f^*(L)$ for a ligand L^- is given by $f^*(L) = f(L) + \delta$.

At present, we have very little data with which these tentative suggestions can be tested. The correlations of spectrochemical constant, where known,[81] with binding energy and with J_{HD} are shown in Figure 10, in which δ for Cl^- (and for any X^- ion) has been assigned the value 0.20 to bring about approximate agreement with J_{HD}. Insofar as these correlations are valid, they also indirectly imply the further correlations discussed above. We cannot place too much reliance on these at present, owing to the paucity of data. However, they are suggestive of linkages between established chemical and spectroscopic properties of ligands which are qualitatively in the correct direction, and which may serve as an approximate guide to properties of as yet unknown

(80) Barfield, M.; Collins, M. J.; Gready, J. E.; Sternhell, S.; Tansey, C. W. *J. Am. Chem. Soc.* **1989**, *111*, 4285.

(81) Lever, A. B. P. *Inorganic Electronic Spectroscopy*; Elsevier: Amsterdam, 1984.

(82) Gerloch, M.; Slade, R. C. *Ligand-Field Parameters*; Cambridge University Press: Cambridge, 1973.

structures. One notes, for example, that the suggested correlation between large spectrochemical constant and low stability of the η^2-H_2 complex is in accord with the experimental fact that a CN^- ($f(L) = 1.7$[81]) complex is too unstable to be characterized[23] in solution.

Future detailed calculations will bring such attempted correlations into sharper focus. We have not made any systematic study of the effects of replacing the NH_3 ligands, although we have reported earlier[22] that a calculation at the SCF level for an Os(II) complex with $2CO + 3PH_3$ ligands, analogous to the structure of the W complex of ref 3, yielded only one (η^2-H_2) potential minimum, as in Figure 9C. There is clearly much to be done before the factors governing geometry and properties of these novel systems are fully understood.

Acknowledgment. J.S.C. gratefully acknowledges the support of the Australian Research Council. We are most grateful to Prof. H. Taube (Stanford University) for providing us with unpublished results, and for extensive discussions.

Registry Numbers Supplied by Author: $[Os(NH_3)_4(CH_3)_2CO(\eta^2\text{-}H_2)]^{2+}$, 136658-64-5; $[Os(NH_3)_4H_2O(\eta^2\text{-}H_2)]^{2+}$, 136629-56-6; $[Os(NH_3)_4CH_3COO(\eta^2\text{-}H_2)]^{+}$, 147831-48-9; $[Os(NH_3)_4Cl(\eta^2\text{-}H_2)]^{+}$, 136629-54-4; $[Os(NH_3)_4C_5H_5N(\eta^2\text{-}H_2)]^{2+}$, 136629-48-6; $[Os(NH_3)_4CH_3CN(\eta^2\text{-}H_2)]^{2+}$, 136629-50-0.